Pergamon

Cement and Concrete Research, Vol. 27, No. 10, pp. 1489–1499, 1997

0008-8846/97 $17.00 + .00

PII S0008-8846(97)00170-1

# NUMERICAL MODELLING OF AUTOGENOUS SHRINKAGE OF HARDENING CEMENT PASTE

**E.A.B. Koenders and K. van Breugel**
Delft University of Technology, Delft, The Netherlands

(Refereed)
(Received December 11, 1996; in final form August 5, 1997)

## ABSTRACT

Hardened cement paste is a porous material. As hydration proceeds, pores become emptied and the relative humidity reduces. This reduction of the relative humidity goes along with a reduction of the pressure in the emptied pore space. Thermodynamic equilibrium requires an increase of the surface tension in the boundary layer that develops at the inner pore wall area. For validation of the model, experiments have been carried out. Good agreement is reached between the numerical simulations and the results obtained from experiments. © *1997 Elsevier Science Ltd*

## Introduction

The pore volume of cement paste is generally defined as the initial paste volume minus the volume of the solid material. From this, the porosity is defined as the ratio between the pore volume and the initial paste volume. The porosity is classified in different categories of pore diameters that range between certain limits. For neat cement paste, the pore system consists of pores with diameters ranging between 10 Å to $10^7$ Å (1). A distinction is made between three types of pores: gel pores, capillary pores, and air voids. Several authors have proposed upper and lower boundaries for these three types of pores. There exists no general agreement on the boarder limits that should be used. As an example, Table 1 provides an overview of the different pore types and range limits, as proposed by Young (1).

The porosity of cement paste consists of pores that exhibit a certain pore size distribution. In this paper, a mathematical description will be proposed that simulates this pore size distribution. With this, pore fractions of a certain diameter represent a certain pore volume in the paste. The summation of all these fractions again lead to the total pore volume. With this formulation, the moisture state in the hardening paste can be described in detail. This is necessary for modelling the volumetric changes of hardening cement paste.

It is possible to reach thermodynamic equilibrium in the capillary pore system. This is a continuously changing state of equilibrium that is driven by the degree of hydration. The model as it is proposed in this paper equilibrates the relative humidity in the emptied pore space with the thickness of the surface layer at the pore walls and with the surface tension in this layer. This equilibrium can be established iteratively.

To come to the volumetric changes of the hardening microstructure, the model originally proposed by Bangham in 1931 will be adopted (2). This model relates the volumetric changes

TABLE 1
Classification of pores in cement paste (after (1))

| Type | Diameter [μm] | Description | Role of water |
|---|---|---|---|
| Capillary pores | 10-0.002 | Macro pores | Accessible for water and able to transport water |
| Gel pores | <0.002 | Micro pores | Not accessible for water. Not able to transport water |

of the continuously changing microstructure to the changes of the surface tension in the surface layer that has been formed at the pore walls. This appeared to be a linear relationship.

For the determination of the evolution of the microstructure of cement-based materials, the numerical simulation program HYMOSTRUC is used. This program has the potential to simulate and predict the microstructural development as a function of the particle size distribution and the chemical composition of the cement, the water/cement ratio, and the temperature (3).

The model discussed in this section has been implemented in the HYMOSTRUC program (4). The volumetric changes of experiments on cement pastes with different water/cement ratios and with cement of different fineness, as well as tests taken from literature are simulated with the proposed model.

## Pore structure

### Modelling Approach

During the hydration process, cement paste changes gradually from a viscous liquid to a porous building material. The pore space in this material follows a certain distribution. From this distribution, the relationship is known between the pore diameter and the pore space that is occupied by all the pores of this particular dimension. In HYMOSTRUC, the pore-size distribution is described mathematically (see Fig. 1) (5) by the function:

$$V_{\text{por},\leq\phi} = a\ln\left(\frac{\phi}{\phi_0}\right) \tag{1}$$

In this description of the pore space, $V_{\text{por},\leq\phi}$ is the capillary pore volume of all pores with diameter $\leq\phi$ [μm], $\phi_0$ the minimum capillary pore diameter and $a$ the constant representing the increase of the pore space with respect to the pore diameter. The pore volume formed by pores smaller than $\phi_0 = 0.002$ μm, e.g., the gel porosity, is not included in this formulation. The maximum pore diameter $\phi_{\text{por}}$ that is involved in the pore space at a degree of hydration $\alpha(t)$ can be recalculated from Eq. 1 as follows:

$$\phi_{\text{por}}(\alpha(t)) = \phi_0\exp\left(\frac{V_{\text{por}}(\alpha(t))}{a}\right) \tag{2}$$

The total pore space $V_{\text{por}}$ is considered to be the product of two contributions: the volume that is occupied by the capillary water $V_{\text{cap}}$ and an additional volume occupied by a volume that

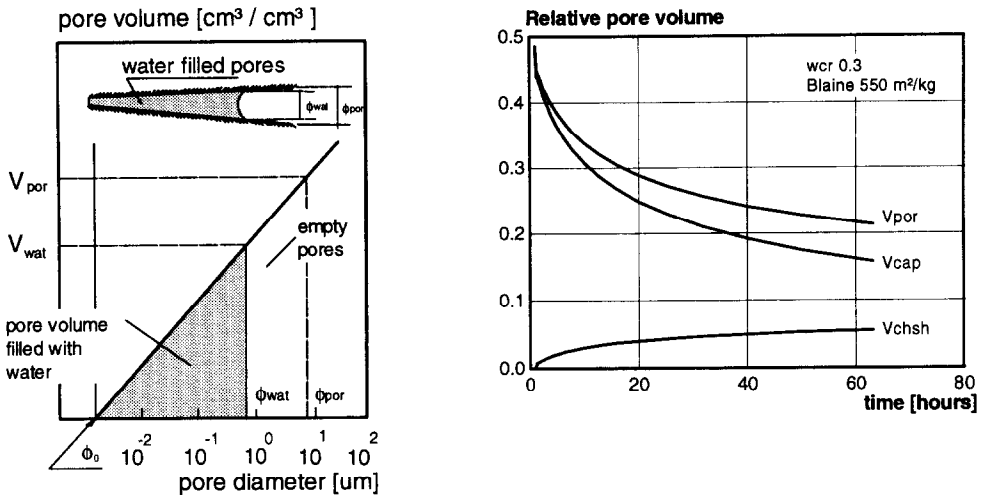


FIG. 1.

Left: Schematical representation of the pore size distribution according to Eq. 1. Right: Different volume components considered in the pore model.

is the result of chemical shrinkage $V_{chsh}$. The relative contributions of both volumes will change due to changes of the microstructure as a result of the hydration process. Finally, this can be denoted as follows (see Fig. 1):

$$V_{por}(\alpha) = V_{cap}(\alpha) + V_{chsh}(\alpha) \tag{3}$$

Accordingly, the pore structure model can be represented as shown schematically in Figure 1 (left). The pore diameters range between $\phi_0$ and $\phi_{por}$. The inner pore wall area is considered to be covered by a thin adsorption layer of water molecules. The thickness $\Gamma$ of this layer depends mainly on the relative humidity in the pore system. If the capillary pores become emptied gradually during hydration, the relative humidity in the pore system will decrease. Accordingly, the thickness of the adsorption layer will decrease too. This behaviour has been examined experimentally be Hagymassy. The results of his findings are presented in Fig. 2 (left). From the results, it appears that the inner pore walls are covered with an adsorption layer of a thickness that ranges roughly between 2 and 6 layers of 3 Å each (Fig. 2, right). It is assumed that the adsorbed water volume $V_{ad}$ that is occupied by the adsorption layer goes at the cost of the free capillary pore water volume $V_{free}$.

$$V_{free}(\alpha) = V_{cap}(\alpha) - V_{ad}(\alpha) \tag{4}$$

Depending on the relative humidity in the pore system, this will effect the amount of capillary water that is available for further hydration. The approach as it has been proposed up until now can be adopted for modelling the pore structure. The only unknown parameter that remains is the pore constant $a$. The value of this parameter can be determined from experimental data. Book keeping a data base that contains this constant for different types of mixtures is a serious option to achieve an adequate description of the pore structure. However, there exists an alternative way to obtain the pore constant $a$. It is possible to

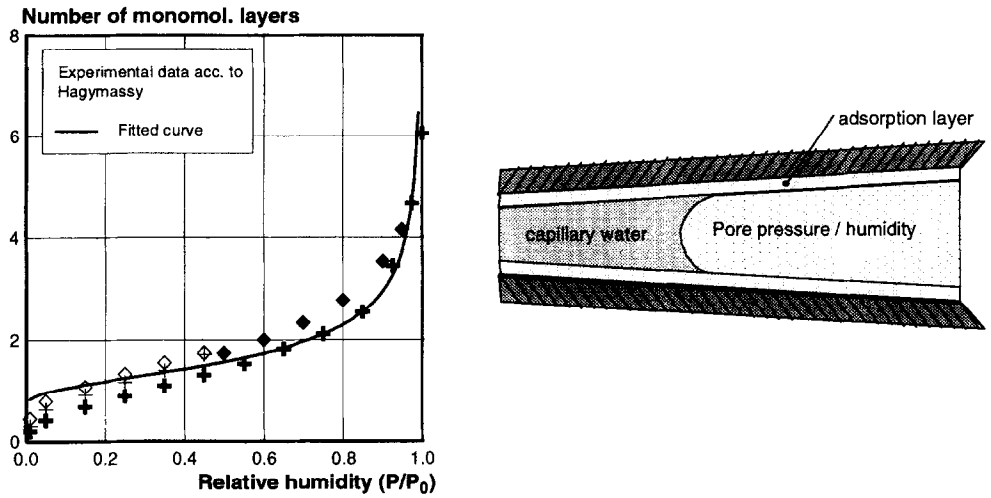


FIG. 2.
Left: Number of adsorption layers vs. relative humidity in the pore system. Right: Schematic view of the state of water in the pore system.

determine the pore structure constant $a$ from a random particle structure. The different ways to determine the pore structure constant $a$ will be elucidated in detail in the next section.

## Pore Structure Constant $a$ Determined from Experiments

The dimensionless parameter $a$ can be derived from measurements by dividing the intrudes pore volume by the pore range. This can be carried out with the help of Eq. 1 and assuming the minimum capillary pore to be equal to 0.002 μm. An extended literature study found that this parameter ranges between 0.05 (coarse cement) and 0.11 (fine cement) depending on the type and fineness of the cement that is used. From this information, the pore structure can be modelled in a proper way (Eq. 1).

In Figure 3, pore size measurements (left) (6) are compared with the pore size distribution as modelled according to Eq. 1 (right). From the measurements, it is calculated that the inclination angle $a$ is about 0.08. This value is applied to the model. The agreement between the experimental and simulated results is quite good. It shows also the reduction of the average pore diameter as hydration proceeds.

## Pore Structure Constant $a$ Determined from Random Particle Structure

It is also possible to determine the pore size distribution for a random pore structure. In the extended version of the HYMOSTRUC model, the formation of structure is modelled by an increase of the radii of the spherical cement particles that were parked in space randomly. During hydration, the physical boundaries of the cement particle start to grow and to form a structure. Some particles may become embedded in the outer product layer of larger particles. This procedure results in the formation of a load bearing framework. In Figure 4, two stages of the progress of the hydration process are presented for a cement of medium fineness

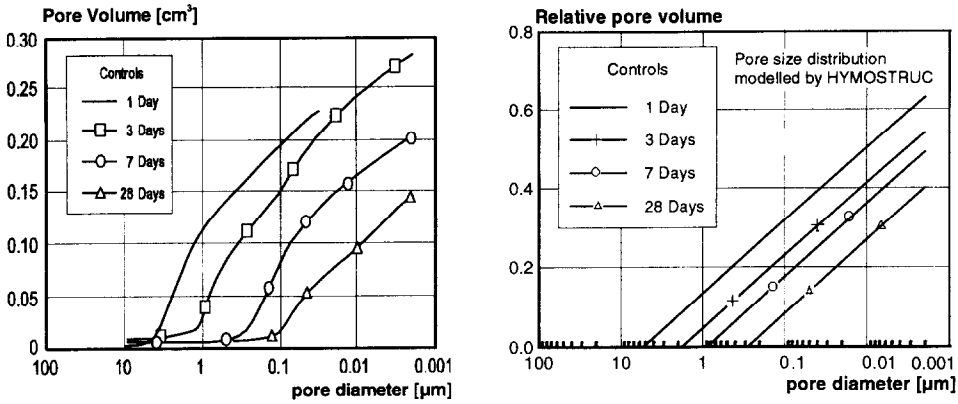


FIG. 3.

Left: Pore size distribution measured by Whiting (6). Right: Pore size distribution according to the proposed model.

(Blaine 420 $m^2/kg$) and a water/cement ratio of 0.3. Initially, if no hydration has taken place, only unhydrated cement particles exist randomly distributed in the mixing water facing the water/cement ratio. It is assumed that the formation of the microstructure starts after the dormant stage has ceased. At that stage, a structure of unhydrated grains and hydration products appear. The distinction between the formed hydration products, called "outer product," and the zone at which the mixing water has penetrated into the cement particle, called "inner product," can be observed from the figure quite clearly. At an arbitrary degree of hydration of 0.1, a microstructure with little formation of hydration products can be observed. However, at a degree of hydration of 0.5, the actually developed hydration products tend to form a dense microstructure. From this structure, the pore space can be recognised (black colour). Most of the pores are closed and surrounded by hydrating cement

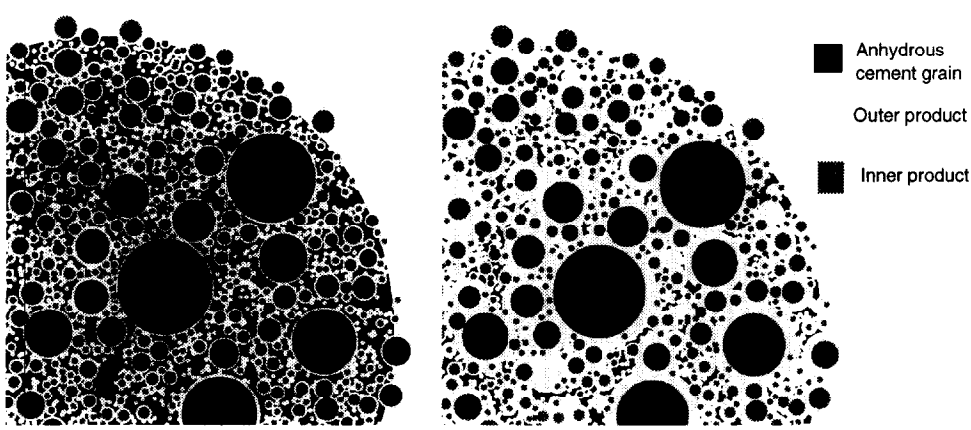


FIG. 4.

Cross section of a random particle structure at $\alpha = 0.1$ (left) and $\alpha = 0.5$ (right), representing a cement paste of medium fineness (Blaine 420 $m^2/kg$) and a water/cement ratio of 0.3. (background colour, black).

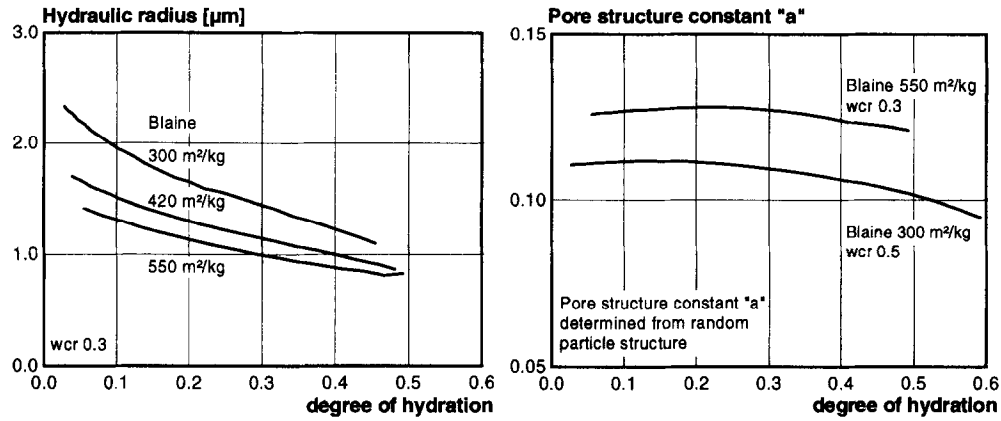


FIG. 5.

Left: Hydraulic radius vs. degree of hydration. Right: Pore structure constant $a$ vs. degree of hydration for two different cement pastes determined from the random particle structure.

particles. The average dimensions of the pores that can be observed range roughly between 1 and 10 μm. However, because the shape of the pores is irregular, is it very difficult to determine a pore size distribution from a real microstructure, as well as from a hardening cement paste model (Fig. 4). Among others, Setzer (7) proposed a procedure to determine the hydraulic radius from the pore volume $V_{por}$ and the pore wall area $A_{por}$. This radius is defined as follows:

$$R_H = \frac{V_{por}}{A_{por}} \tag{5}$$

where $R_H$ is the hydraulic radius. Together with the pore size distribution (Eq. 1) and the minimum diameter of the capillary pore, the hydraulic radius can be determined from the random particle structure (Fig. 5, left). The hydraulic radius changes continuously with progress of the hydration process. The hydraulic radius decreases with increasing degree of hydration. This holds true for the three types of cement with different fineness (Fig. 5). Densification of the microstructure due to the formation of hydration products around the hydrating cement particles will reduce the initial pore volume of the hardening cement paste. Conversely, it will enlarge the inner pore wall area because the average pore diameter decreases. This means that the more hydration products are formed, the more specific surface will be formed that leads to an increase of the inner pore wall area. Assuming that the hydraulic radius represents a weighted pore diameter for the hardening paste, it is possible to determine the pore constant $a$ from the random particle structure. From the hydraulic radius $R_H$ and the pore volume $V_{por}$, and with help of Eq. 1, the pore structure constant $a$ can be calculated. At the right hand side of Fig. 5, the pore structure constant is shown for two different types of cement paste. It appears that the value differs only slightly for both pastes. It also appears that the value is highest for the cement paste that contains fine cement and a low water/cement ratio. A higher value $a$ in Eq. 1 implies that more smaller pores are involved in the microstructure. This is in good agreement with what is generally found by experimental data (finer cement) (8).

## Thermodynamic Equilibrium in the Pore Space

At a certain stage of the hydration process, some pores are partly filled with fluid and partly with air. This implies that there exists a water/vapour interface layer in these pores between the fluid and the air. Physically, this system can be considered as a three phase system, e.g., capillary water (fluid) – interface – air (gas). This can also be described in terms of the bulk phases. These are the free capillary water, the adsorption layer, and the gas filled pore space. The composition of the interface volume will usually differ from the other two bulk phases. Therefore, it appears to be useful to express the composition of the surface phase (adsorption layer) in terms of mole or weight fractions. A macroscopic definition of adsorption can be derived by using the Gibbs (9) theory. This theory is based on a three-phase system consisting of a dividing surface layer and two additional phases that are considered to be homogenous up to the geometrical dividing surface (see also Fig. 2, right). In the Gibbs model, initially the thickness of the interface is taken as zero, whereas in a real system this interface layer has a finite thickness. Assume $c_i$ as the concentration of component i, in moles per unit volume. If so, the number of moles in the liquid phase and the gas (air) phase can be denoted by $n_i = c_i \cdot V_i$. Considering the capillary pore system to be a closed system that contain $n$ moles, conservation of mass requires for the interface:

$$n_\sigma = n - n_{\text{liquid}} - n_{\text{gas}} \tag{6}$$

where $n_\sigma$ is the number of molecules adsorbed to the pore wall area, $n$ is the total number of moles involved in the total system, $n_{\text{liquid}}$ is the number of moles in the liquid phase (capillary water times its concentration $c$), and $n_{\text{gas}}$ is the number of moles present in the gas phase of the system (air in pores)). The number of moles per unit area that is adsorbed to the pore wall area can be determined by:

$$\Gamma = \frac{n_\sigma}{A_{\text{por}}(\alpha(t))} \tag{7}$$

where $A_{\text{por}}(\alpha(t))$ is the total pore wall area (see Fig. 1). Considering the three-phase system as described above, the mechanical work $W$ that occurs for a infinitesimal phase change of the capillary system can be formulated as follows:

$$dW = d(pV) + d(\sigma A) \tag{8}$$

where $p$ is the pressure in the system, $V$ is the volume of the capillary water, $\sigma$ is the surface tension, often called "free surface energy," and $A$ is the surface area that is submitted to the surface tension. If $dQ$ is the heat that is produced by an infinitesimal change of a mechanical system, then the first principal of thermodynamics leads to:

$$dQ = dU + dW \tag{9}$$

where $dU$ is the internal energy in the system and $dW$ the work carried out by the system. In a closed system an infinitesimal change of $dQ$ can be written as $dQ = SdT$; where $dT$ is the absolute temperature increment of the system and $S$ the entropy. If the temperature remains constant during an infinitesimal phase change, this latter term becomes zero. This leads to a more simplified formulation of the description of the thermodynamic equilibrium in the pore system. Conservation of work for a closed capillary pore system leads to the following expression for the change of the surface tension with respect to the pressure:

$$\frac{\partial \sigma}{\partial p} = \frac{RTn_{\sigma}}{pA(\alpha(t))} \tag{10}$$

with $R$ the general gas constant and $T$ the absolute temperature. Substitution of Eq. 7 in Eq. 10 and integration leads to the basic Eq. 11, which describes the relationship between surface tension and the pressure in the pore system.

$$\sigma = RT\int \Gamma d\ln(p) \tag{11}$$

At the early stage of the hydration process, it is assumed that all pores are completely filled with water (disregarding air voids). At this particular stage, the relative humidity in the pore system (space) is equal to 100%. With progress of the hydration process, water becomes consumed. Part of the pores remain filled with capillary water and part of the pores become empty. At this stage of hydration, the relative humidity in the emptied pore space will drop below 100%. In HYMOSTRUC, the relative humidity in the pore space is modelled by the Kelvin equation (9–11).

$$\ln\left(\frac{p}{p_0}\right) = \frac{-4\sigma}{RT\gamma_w\phi_{wat}} \tag{12}$$

in which $\phi_{wat}$ is the widest pore diameter that is still completely filled with water (see Fig. 1). The Kelvin equation describes the variation of the pore pressure as a function of the pore diameter $\phi_{wat}$ and also as a function of the surface tension $\sigma$. A further reduction of the capillary volume due to hydration will decrease the relative humidity in the pore system. This will influence the pore diameter $\phi_{wat}$ as well as the surface tension in the adsorption layer.

## Towards Autogenous Deformation

The volumetric changes of hydrating cement paste is a result of the reduction of the relative humidity in the pore system (self-desiccation). It was Bangham (12) who related the external deformation of coal to the surface tension in the adsorption layer formed to the inner pore wall area. In several papers, he used the adsorption equation of Gibbs to describe this phenomenon. Bangham used his theory to point out that, with solid as opposed to liquid surfaces, the surface energy, representing the work spent for the formation of a unit of new surface, must thermodynamically be in equilibrium with the pressure. In his theory, his considered the three-phase system as discussed in the previous section. Next, he found that the expansion of coal could be related linearly to the change of the surface energy that appears in the adsorption layer. This approach has also been proposed for hardening cement paste by, among others, Wittmann (13). As far as hardening cement paste is concerned, the material properties change continuously with the elapse of time. Therefore, the proposed relation must be considered incrementally and can be formulated as follows:

$$\frac{\partial \varepsilon_a}{\partial t} = \lambda \cdot \frac{\partial \sigma}{\partial t} \tag{13}$$

where $\partial\epsilon_a$ is the increment of autogenous shrinkage, $\partial\sigma$ is the surface tension increment (see Eq. 11) and $\lambda$ is a proportionality factor. In fact, this constant is the compliance modulus of

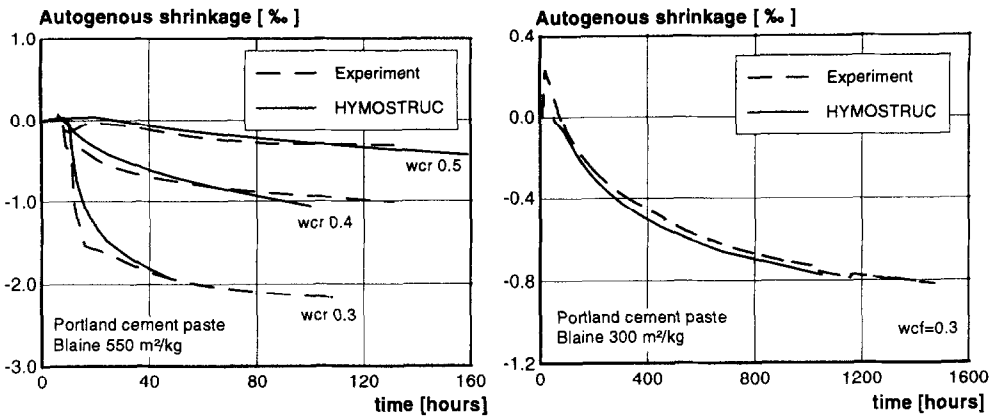


FIG. 6.
Autogenous shrinkage of cement paste vs. time. Left: Fine cement (high hydration rate) with different water/cement ratios. Right: Coarse cement (low hydration rate).

the hardening material (cement paste). According to Bangham, coal would swell proportional to the decrease of the free surface energy. In general, for hardening cement paste, the opposite behaviour is observed, viz. cement paste shrinks proportional to a increase of the free surface energy.

The proportionality factor $\lambda$ that relates the microstructural deformation to the surface tension in the pore system was formulated more or less similarly by several authors (14–17). As was proposed by Bangham, the constitutive relation, which describes the relationship between the deformation of the microstructure and the tension in the adsorption layer, yields:

$$\lambda = \frac{\Sigma \cdot \rho_{pa}}{3E} \tag{14}$$

with: $\Sigma$ = pore wall area of the empty pores
Note: $\Sigma = \Sigma(\alpha(t)) = A_{por}(\alpha(t)) - A_{wat}(\alpha(t))$
$\rho_{pa}$ = specific mass of the cement paste
$E$ = modulus of elasticity of the cement paste
Note: $E = E(\alpha(t))$
As can be noticed from this relation, the pore wall area, the specific mass of the cement paste, and the development of the modulus of elasticity plays an important role for accurate simulation of the volumetric changes of the microstructure (autogenous shrinkage) during the hardening phase.

## Measurements vs. Numerical Simulations

In Figure 6 (left), the autogenous shrinkage is presented as a function of time for a cement paste that contains a cement of high fineness (Blaine 550 $m^2$/kg). Results are shown for a water/cement ratio of 0.3, 0.4, and 0.5. It shows a strong increase of the autogenous shrinkage for a decrease of the water/cement ratio. The largest autogenous shrinkage, ca. 2‰, is measured after about 168 h of hydration for the cement paste with water/cement ratio of 0.3.

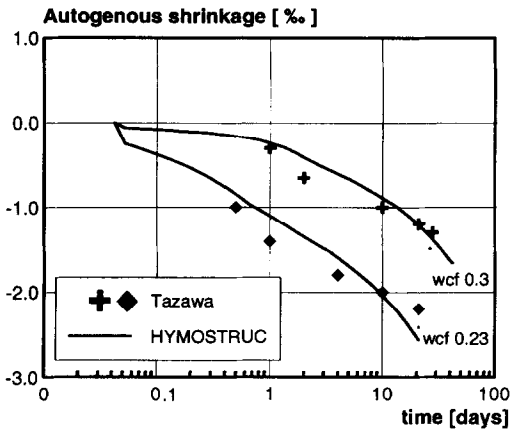


FIG. 7.
Comparison between experiments on cement paste (Blaine 352 $m^2$/kg) carried out by Tazawa and Miyazawa (18) and numerical simulations by HYMOSTRUC.

The very strong increase of the autogenous shrinkage at the beginning of the hardening process can be related to the fact that at this early stage of the hardening process, the elastic modulus has only developed minorly. The volumetric contraction of the microstructure will then experience hardly any restraint of the stiffness of the paste. Consequently, large deformations can easily occur. For higher water/cement ratios, this contraction force will be much smaller so that the volumetric contraction of the microstructure will be less pronounced at that particular stage of the hardening process.

For a cement paste with a ratio of 0.4, much less shrinkage is measured. After 168 h of hardening, a shrinkage value of about 1‰ has been reached. This is a strong reduction (50%) in comparison with the paste that has a water/cement ratio of 0.3. A further increase of the water/cement ratio to 0.5 reduces the autogenous shrinkage again by an other 50%.

In Figure 6 (right), a shrinkage measurement is presented for a cement paste with a cement fineness of 300 $m^2$/kg. Due to this relatively coarse type of cement, the hydration process will develop rather slow. Implicitly, the development of the autogenous shrinkage will develop slowly as well. From the figure it can be observed that the autogenous shrinkage is still increasing after about 1400 h of hardening. This process will proceed until hydration has ceased. The measured volumetric contractions are simulated by the HYMOSTRUC. These simulations are based on the shrinkage model as outlined in the previous sections. The results show a very good agreement. In addition, the early age chemical swelling is not included in the model.

Tazawa (18) has presented his results of an extended experimental study on autogenous shrinkage of cementitious material. Some of his results on plain cement pastes are simulated with the proposed shrinkage model as implemented in HYMOSTRUC. The results are shown in Figure 7. Good agreement has been obtained between the experimental results and the numerical simulations. This holds true for water/cement ratios of both 0.3 and 0.23. The autogenous shrinkage increases to a level of about 1.5‰ for the cement paste with a water/cement ratio of 0.3 and reached a value of about 2.5‰ for the cement paste with a water/cement ratio of 0.23. However, the volumetric contraction of the microstructure may continue as long as hydration goes on.

## Conclusions

Describing the volumetric changes of hardening cement paste on a thermodynamical basis turned out to be quite satisfactory. The proposed model predicts the autogenous deformation of hardening cement paste quite accurately. The numerical simulations are in good agreement with the experimentally obtained results for cement pastes that contain cement of relatively high fineness as well as for pastes that contain a relatively coarse type of cement. This holds true for various water/cement ratios.

In addition, to come to a model to predict the volumetric changes of hardening concrete, internal restraint due to the availability of stiff aggregates has to be taken into account. Composite models as proposed by Counto or Hirsch can be applied for this purpose. However, the internal restraint can also be simulated with the aid of a lattice model (19).

## References

1. J.F. Young et.al., Document prepared by RILEM TC69.
2. D.H. Bangham and N. Fakhoury, The Swelling of Charcoal. Royal Society of London CXXX-(Series A): 81–89 (1931).
3. K. van Breugel, Cem. Concr. Res., Theory (I): 25, 319–331 (1995); Applications (II): 25, 522–530 (1995).
4. E.A.B. Koenders, Simulation of volume changes in hardening cement-based materials, Ph.D. Thesis, Delft University of Technology, The Netherlands, 1977.
5. K. van Breugel, Simulation of hydration and formation of structure in hardening cement-based materials, Ph.D. Thesis, 1991.
6. D. Whiting and E. Kline, Cem. Concr. Res. 7, 53–60 (1977).
7. M.J. Setzer, Oberflächenenergie und Mechanische Eigenschaften des Zementsteins, p. 113, TU München, München, 1972.
8. R.F. Feldman and H. Cheng-yi, Cem. Concr. Res. 15, 766–774 (1985).
9. R. Defay, I. Prigogine and A. Bellemans, Surface Tension and Adsorption, Longmans London, London, 1966.
10. W. Grün and H.R. Grün, Zement-Kalk-Gips 11, 541–520 (1961).
11. K. van Breugel, Artificial Cooling of Hardening Concrete, Delft University of Technology, Research report concrete structures, 5-80-9, 1980.
12. D.H. Bangham, The Gibbs Adsorbtion Equation and Absorbtion on Solids, Gurney and Jackson, London, 1937.
13. F. Wittmann, Physikalische Messungen an Zementstein. TU München, München, 1968.
14. D.H. Bangham and F.A.P. Maggs, The Strength and Elastic Constants of Coal in Relation to their Ultra-fine Structure, The British Coal Utilisation Research Association, The Royal Institution, London. 1944.
15. D.J.C. Yates, Proc. Royal Soc. London 224, 526–543 (1954).
16. K.H. Hiller, J. Appl. Phys. 35, 1622–1628 (1964).
17. V.S. Ramachandran, R.F. Feldman, and J.J. Beaudoin, Concrete Science, Treatise on Current Research, Division of Building Research, National Research Council, Canada, Heyden, 1981.
18. E. Tazawa and S. Miyazawa, 9th Int. Conf. Chem. Cem. New Delhi, IV, 712–718 (1992).
19. K. van Breugel and E.A.B. Koenders, Numerical Simulation of the Effect of Elevated Temperature Curing on Porosity of Cement-Based Systems. MRS-FALL Conference, Boston, USA, 1995.